International Journal of Engineering Inventions
e-ISSN: 2278-7461, p-ISSN: 2319-6491
Volume 15, Issue 6 [June 2026] PP: 74-82

Study on Robust Frequency Regulation of a Single-Area Small Hydropower System Using Sliding-Mode Control

Nguyen Duy Trung[1], Hoang Van Hoat[2], Le Cong Viet[1], Nguyen N. – Khoat[1], Pham Van Nam[1]
[1]*Faculty of Control and Automation, Electric Power University, Hanoi, Vietnam*
[2]*TTH Vietnam Automation Company, LTD, Hanoi, Vietnam*
Corresponding Author: nknguyenepu@gmail.com

ABSTRACT: *This paper presents a robust speed-control strategy for a single-area small hydropower plant under load-frequency regulation. A reduced-order governor-turbine-generator model is formulated with frequency deviation, guide-vane position, mechanical power and integral-frequency states. To overcome the slow recovery and residual steady-state error of conventional droop, PI and PID governors, a continuous integral sliding-mode controller is developed with a boundary-layer hyperbolic tangent function and practical gate saturation. The proposed method is evaluated in MATLAB under three sequential load disturbances and under ±20% hydropower parameter variations. Comparative simulations show that the proposed sliding-mode controller gives the smallest peak frequency deviation, IAE, ISE, ITAE and final-step settling time. Relative to the PID governor, the proposed method reduces the IAE by approximately 74.8% and the final-step settling time by approximately 72.5%, while keeping the guide-vane command bounded and smooth. The results confirm that the proposed controller is a simple, reproducible and robust candidate for speed regulation of isolated or weak-grid small hydropower units.*

Keywords: *small hydropower plant; load-frequency control; speed governor; sliding mode control; single-area power system; MATLAB simulation.*

Date of Submission: 06-06-2026 Date of acceptance: 16-06-2026

NOMENCLATURE

Symbol	Description	Unit
A, B, E	State, control-input and disturbance matrices	compatible state-space units
D	Load damping coefficient	p.u./Hz
Δf	Frequency deviation	Hz
ΔP_L	Load-power disturbance	p.u.
ΔP_m	Mechanical power deviation	p.u.
Δx_g	Governor/guide-vane position deviation	p.u.
M	Equivalent inertia constant	p.u.·s/Hz
s	Sliding variable	controller-dependent
T_g, T_t	Governor and turbine time constants	s
u	Control input or guide-vane command	p.u.
z	Integral of frequency deviation	Hz·s
φ	Boundary-layer thickness	same as s
IAE, ISE, ITAE	Integral performance indices	IAE: Hz·s; ISE: Hz²·s; ITAE: Hz·s²

I. INTRODUCTION

Small hydropower plants are increasingly deployed for rural electrification, local renewable generation and distribution-level support. In isolated or weak-grid operation, the plant must rapidly balance mechanical power and load demand to preserve frequency quality. The dynamic behavior of a hydropower governor is strongly affected by water inertia, gate limits and turbine lag; therefore, speed regulation cannot be evaluated only by steady-state droop performance. The hydropower modelling and control background reported in [1]-[8] shows that even simplified benchmark models are useful for controller screening before detailed nonlinear studies.

Classical load-frequency control (LFC) methods include droop governors, integral controllers, PID-based regulators, fuzzy controllers and metaheuristic tuning [1]-[6], [24]-[32]. These methods are attractive because they are easy to tune and implement. However, their closed-loop performance may degrade when the hydropower parameters vary, when several load steps occur in a short time, or when gate saturation limits the available control action. The problem is more critical in small hydropower systems because the equivalent inertia can be low and the plant may operate far from a strong interconnected grid.

Sliding mode control (SMC) provides a direct robustness mechanism against bounded disturbances and parameter uncertainty [9]-[15]. Recent studies on hydro-turbine governing systems and hydraulic generator regulating systems have investigated integral SMC, terminal SMC, fuzzy SMC and disturbance-observer-based SMC [16]-[23]. These studies demonstrate the potential of SMC, but many formulations are nonlinear, high-order or difficult to reproduce in a compact MATLAB benchmark for single-area small hydropower speed regulation.

The research gaps addressed in this paper are: (i) a lack of concise single-area small hydropower studies where droop-P, PI, PID and SMC are compared under identical saturation and disturbance conditions; (ii) insufficient presentation of editable scientific equations and reproducible simulation code for the governor-turbine-generator benchmark; and (iii) limited discussion of robustness under simultaneous parameter variations in small hydropower speed-control applications.

The main contributions are as follows. First, a compact state-space model is formulated for a single-area small hydropower speed-control system with an integral frequency state. Second, a continuous integral SMC law is developed using a smooth boundary-layer function to reduce chattering. Third, a reproducible MATLAB all-in-one simulation is provided to compare droop-P, PI, PID and SMC controllers under the same load profile and gate saturation. Fourth, high-resolution figures and quantitative indices are used to show that the proposed SMC provides the best overall dynamic performance in the tested scenarios.

II. CONTROL METHODOLOGY

A. Single-area small hydropower model

Fig. 1 shows the considered speed-control and LFC structure. The model retains the dominant generator-load swing, servo-governor and hydraulic turbine dynamics. The generator-load frequency dynamics are given by Eq. (1).

$$M\frac{d\Delta f(t)}{dt} = \Delta P_m(t) - D\Delta f(t) - \Delta P_L(t) \tag{1}$$

The simplified servo-governor and turbine dynamics are expressed by Eqs. (2) and (3), respectively.

$$T_g\frac{d\Delta x_g(t)}{dt} = -\Delta x_g(t) + u(t) \tag{2}$$

$$T_t\frac{d\Delta P_m(t)}{dt} = -\Delta P_m(t) + \Delta x_g(t) \tag{3}$$

To guarantee zero steady-state frequency error after load changes, the integral state is introduced in Eq. (4). The complete state vector is defined in Eq. (5).

$$\frac{dz(t)}{dt} = \Delta f(t) \tag{4}$$

$$x(t) = \left[\Delta f(t) \;\; \Delta x_g(t) \;\; \Delta P_m(t) \;\; z(t)\right]^T \tag{5}$$

Using Eqs. (1)-(5), the state-space form used in the simulations is written as Eq. (6), with matrices A, B and E defined in Eq. (7).

$$\dot{x}(t) = Ax(t) + Bu(t) + E\Delta P_L(t) \tag{6}$$

$$A = \begin{bmatrix} -D/M & 0 & 1/M & 0 \\ 0 & -1/T_g & 0 & 0 \\ 0 & 1/T_t & -1/T_t & 0 \\ 1 & 0 & 0 & 0 \end{bmatrix}, \quad B = \begin{bmatrix} 0 \\ 1/T_g \\ 0 \\ 0 \end{bmatrix}, \quad E = \begin{bmatrix} -1/M \\ 0 \\ 0 \\ 0 \end{bmatrix} \tag{7}$$

The simulation imposes the practical gate saturation $u_{min} \le u \le u_{max}$ and uses the three-step load disturbance defined later in Eq. (14).

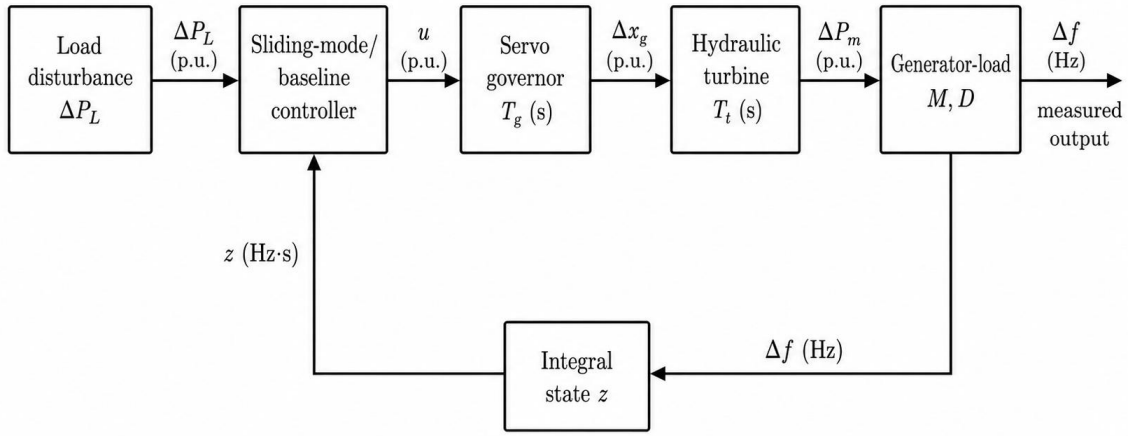

Fig. 1. Single-area small hydropower speed-control and load-frequency regulation structure

B. Baseline controllers

The droop-P, PI and PID controllers in Eq. (8) are implemented as baseline governors. The derivative term in the PID controller is computed from the model-based frequency derivative to avoid noisy numerical differentiation. All controllers use the same saturation limits.

$$\begin{aligned} u_P(t) &= -K_P \Delta f(t), \\ u_{PI}(t) &= -K_P \Delta f(t) - K_I z(t), \\ u_{PID}(t) &= -K_P \Delta f(t) - K_I z(t) - K_D \frac{d\Delta f(t)}{dt}. \end{aligned} \tag{8}$$

C. Proposed continuous integral sliding-mode controller

The proposed controller uses the sliding surface in Eq. (9). Unlike a pure frequency-error surface, Eq. (9) includes the integral state, guide-vane state and turbine mechanical-power state; therefore, it reflects the internal hydropower dynamics instead of reacting only to the measured frequency deviation.

$$s(t) = c_f \Delta f(t) + c_z z(t) + c_g \Delta x_g(t) + c_m \Delta P_m(t) \tag{9}$$

The continuous sliding-mode command is selected as Eq. (10). The hyperbolic tangent term approximates the discontinuous sign function inside a boundary layer with thickness φ. This choice preserves robustness while avoiding severe chattering in the guide-vane command.

$$u_c(t) = -k_f \Delta f(t) - k_i z(t) - k_g \Delta x_g(t) - k_m \Delta P_m(t) - K_s \tanh\left(\frac{s(t)}{\phi}\right) \tag{10}$$

$$u(t) = \mathrm{sat}_{[u_{\min}, u_{\max}]}\big(u_c(t)\big) \tag{11}$$

For the standard reaching analysis, the Lyapunov candidate in Eq. (12) is used. If the lumped matched uncertainty in the sliding dynamics is bounded and the switching gain is sufficiently large, the inequality in Eq. (13) holds outside the boundary layer.

$$V(t) = \frac{1}{2} s^2(t) \tag{12}$$

$$\dot{V}(t) = s(t)\dot{s}(t) \le -\eta |s(t)|, \qquad \eta > 0 \tag{13}$$

Therefore, s(t) reaches a small neighborhood of zero and the frequency error is driven to a bounded neighborhood whose size depends on φ. This practical stability property is appropriate for small hydropower speed regulation, where smooth guide-vane movement and bounded actuation are required. Fig. 2 summarizes the algorithm implemented in MATLAB.

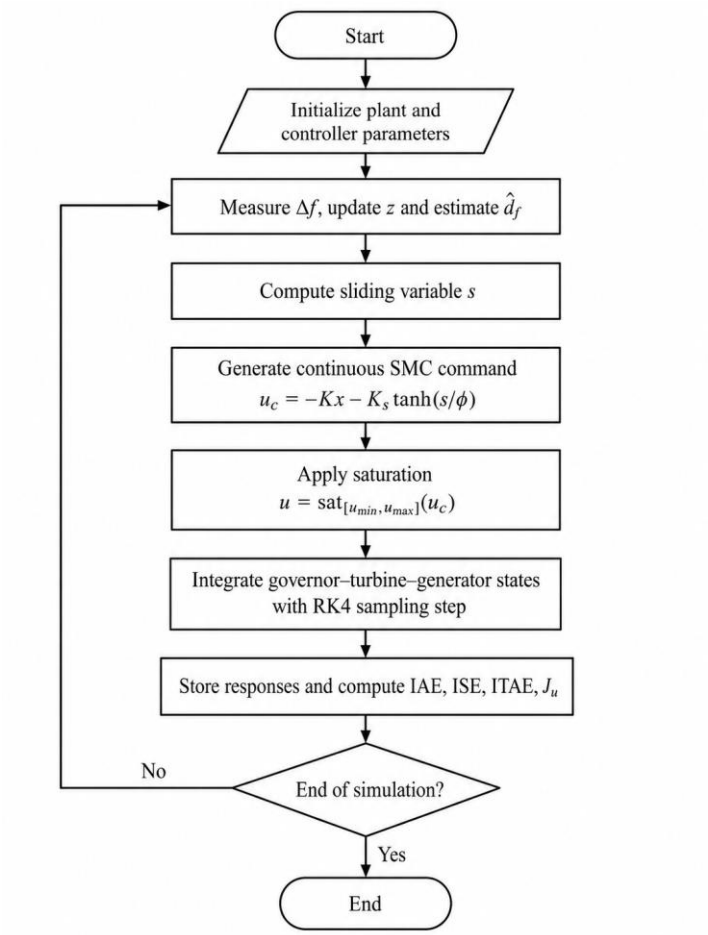

Fig. 2. Flowchart of the proposed sliding-mode speed-control algorithm

Table 1. Nominal parameters of the single-area small hydropower benchmark

Parameter	**Value**
Equivalent inertia M	8.0 p.u.s
Load damping D	1.2 p.u./p.u.
Governor time constant T_g	0.25 s
Turbine time constant T_t	1.10 s
Gate saturation	$-0.35 \le u \le 0.35$ p.u.
Simulation time	180 s
Sampling step	0.01 s

D. Disturbance profile and performance indices

The disturbance scenario consists of three load variations given in Eq. (14). This profile is selected to test the controller under an initial load increase, a second load increase and a later load release.

$$\Delta P_L(t) = 0.05H(t-2) + 0.03H(t-60) - 0.025H(t-120) \quad (14)$$

The quantitative indices used for controller comparison are defined in Eq. (15). The final-step settling time is measured after t = 120 s using the ±0.001 p.u. tolerance band.

$$IAE = \int_0^T |\Delta f(t)|\, dt, \quad ISE = \int_0^T \Delta f^2(t)\, dt,$$
$$ITAE = \int_0^T t\,|\Delta f(t)|\, dt, \quad J_u = \int_0^T \left|\frac{du(t)}{dt}\right| dt. \quad (15)$$

Table 1 lists the nominal benchmark parameters. These values are used to execute numerical simulations in MATLAB to verify the effectiveness of the proposed control strategy.

III. SIMULATION RESULTS

The comparative simulations were performed with the same plant parameters, disturbance profile and gate saturation. The only difference among cases is the controller structure. Thus, Figs. 3-8 and Table 2 provide a fair comparison of droop-P, PI, PID and the proposed SMC.

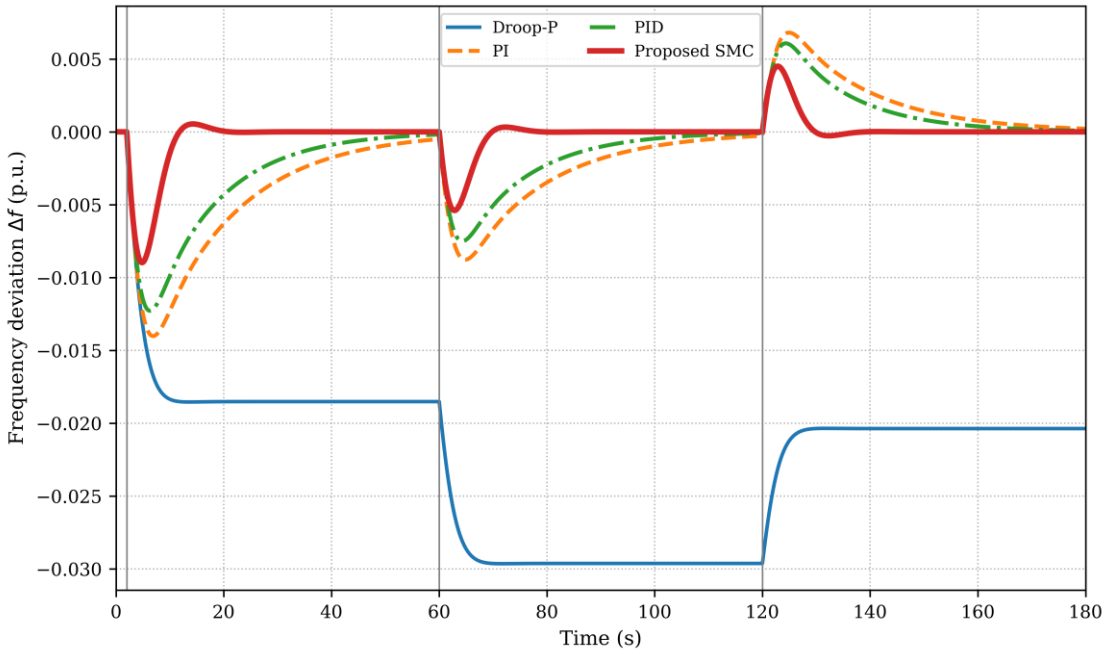

Fig. 3. Frequency response under three-step load disturbance

Fig. 3 shows that the droop-P controller cannot remove the steady-state error after sequential load changes. PI and PID controllers recover the frequency but exhibit larger deviations and slower damping. The proposed SMC gives the smallest frequency excursion and restores the frequency rapidly after each disturbance.

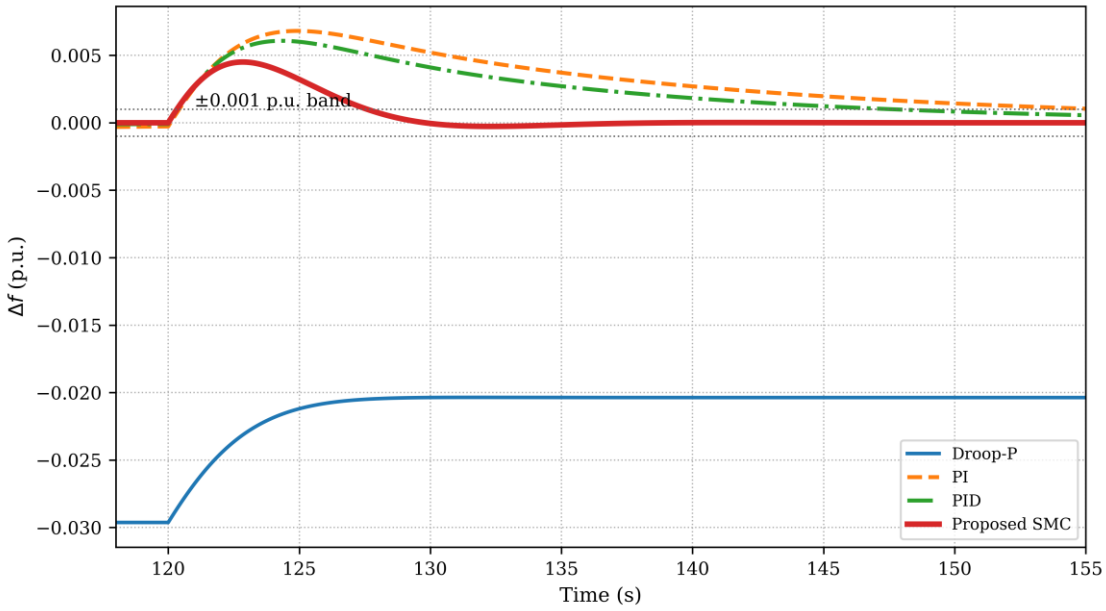

Fig. 4. Zoomed response after the final load variation

Fig. 4 focuses on the final load release at t = 120 s. The proposed SMC enters the ±0.001 p.u. tolerance band in 7.59 s, whereas PID and PI require 27.63 s and 35.65 s, respectively. Droop-P does not satisfy the zero steady-state-error requirement.

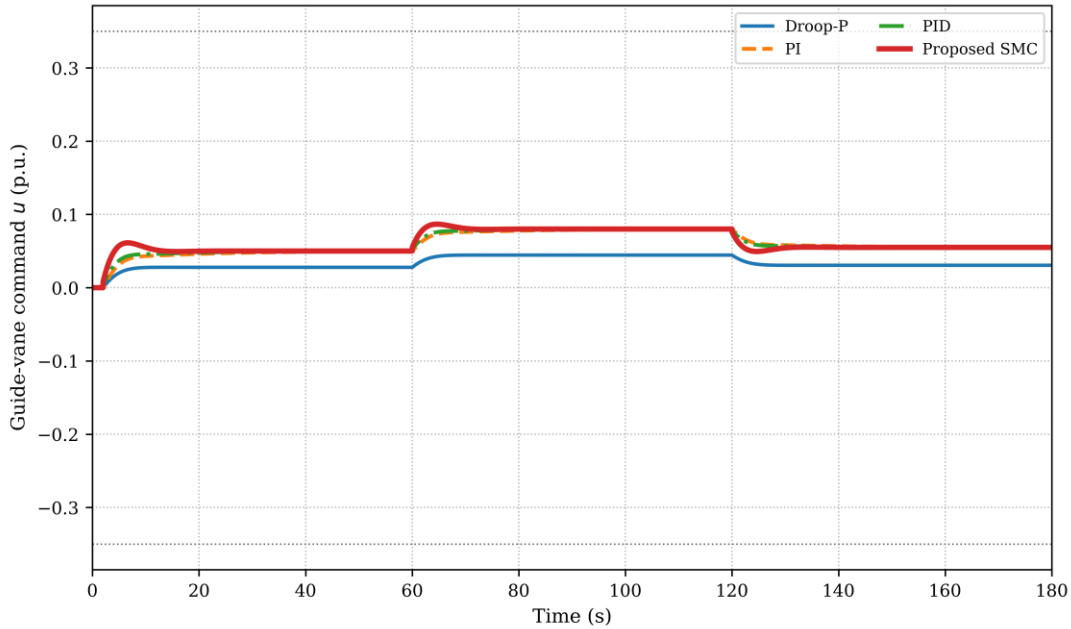

Fig. 5. Governor gate command generated by the compared controllers

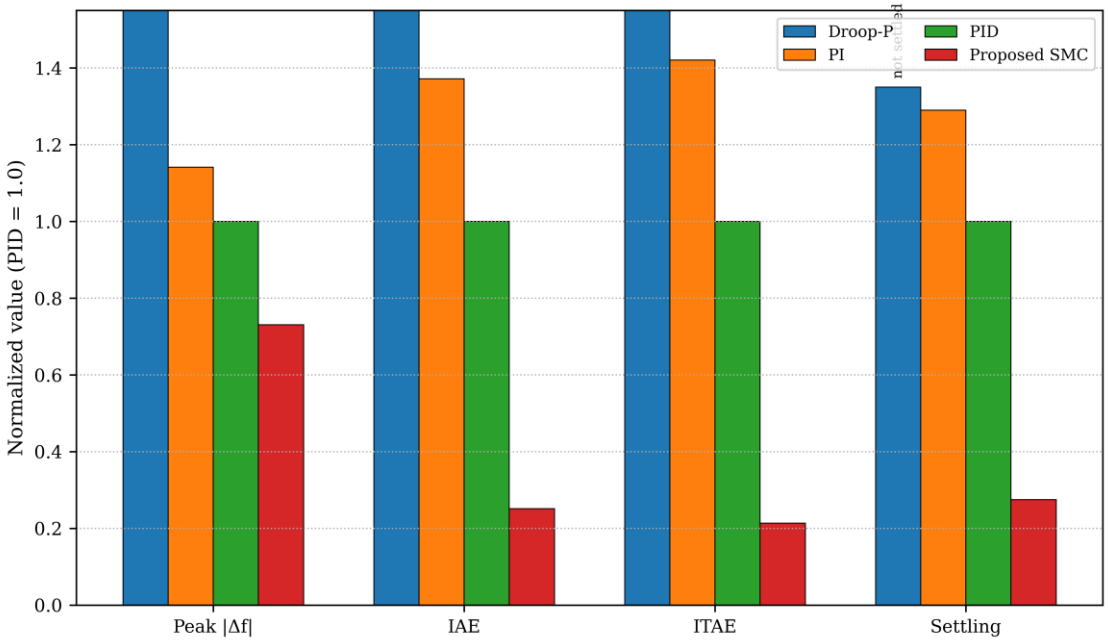

Fig. 6. Normalized performance comparison

Fig. 5 confirms that the SMC command remains within the same saturation limits used by the other controllers. The tanh boundary layer eliminates the high-frequency switching associated with an ideal sign function and produces a smooth guide-vane command.

Table 2. Quantitative comparison of the studied controllers

Controller	Peak |Δf| (p.u.)	Peak |Δf| (Hz)	IAE	ISE	ITAE	Settling (s)
Droop-P	0.029646	1.4823	4.029052	0.096007	377.4482	not settled
PI	0.014020	0.7010	0.571396	0.003653	35.6287	35.65
PID	0.012285	0.6143	0.416621	0.002321	25.0763	27.63
Proposed SMC	0.008975	0.4488	0.104770	0.000510	5.3551	7.59

Table 2 demonstrates that the proposed SMC provides the best values for all frequency-regulation indices. Compared with the PID controller, the SMC reduces the peak frequency deviation by 26.9%, the IAE

by 74.9% and the final-step settling time by 72.5%. These improvements indicate that the proposed controller enhances both transient damping and post-disturbance recovery.

The normalized chart in Fig. 6 visually confirms the quantitative results in Table 2. The proposed SMC has the smallest normalized peak error, IAE, ITAE and settling time. This means that the improvement is not limited to a single metric.

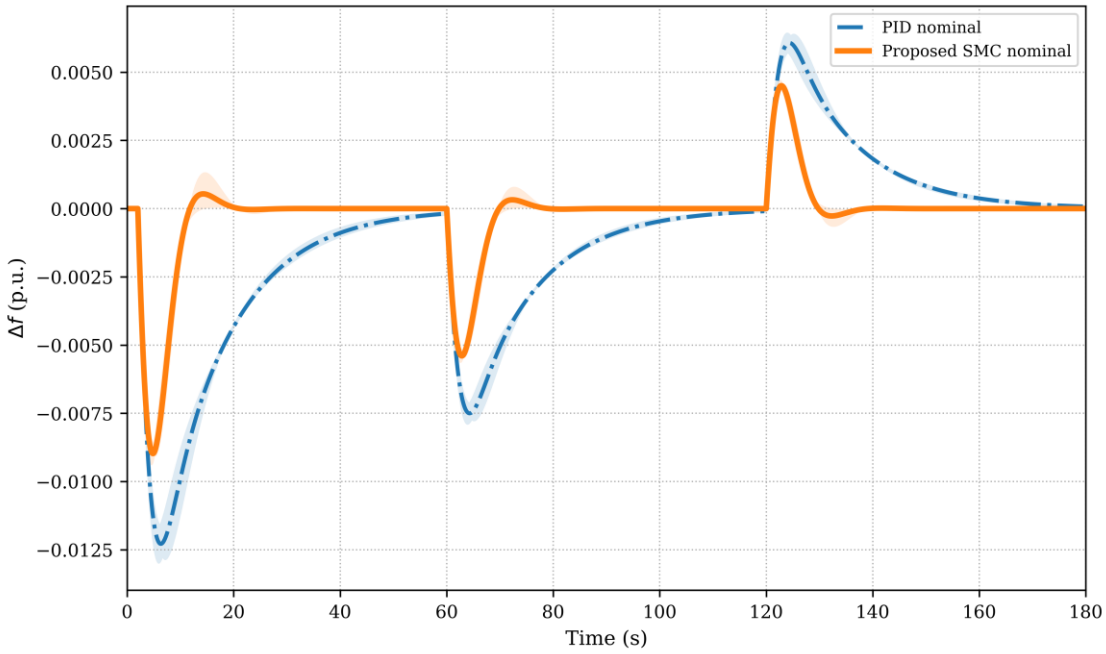

Fig. 7. Robustness check for ±20% hydropower parameter variations

Fig. 7 evaluates robustness when M, D, T_g and T_t are varied simultaneously around their nominal values. The SMC envelope is narrower than the PID envelope, and its nominal response decays faster after each load change. This behavior is consistent with the reaching property in Eq. (13).

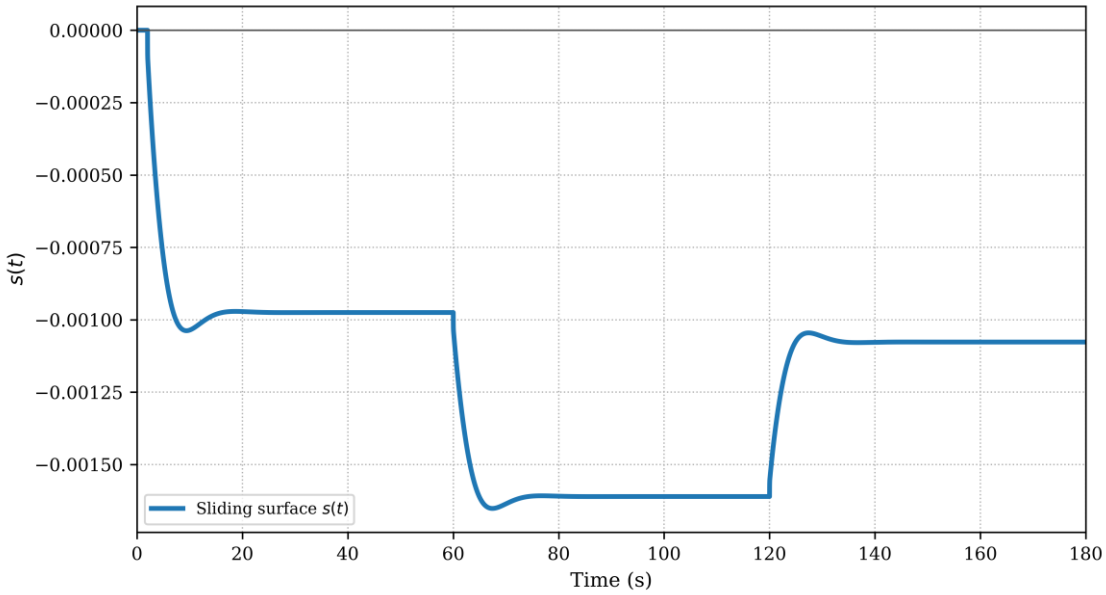

Fig. 8. Sliding-surface convergence of the proposed SMC

Fig. 8 shows that the sliding surface returns to the neighborhood of zero after each disturbance. This result supports the theoretical reaching analysis and explains the fast frequency recovery observed in Figs. 3 and 4.

IV. CONCLUSIONS AND FUTURE WORK

A continuous integral sliding-mode speed controller has been developed for a single-area small hydropower system. The controller uses frequency deviation, integral frequency error, guide-vane position and mechanical-power deviation in the sliding surface, and it applies a tanh boundary layer to avoid high-frequency switching of the guide vane.

The MATLAB simulations show that the proposed SMC achieves the best performance among droop-P, PI, PID and SMC under identical disturbance and saturation conditions. For the selected benchmark, the proposed SMC obtains a peak frequency deviation of 0.008975 p.u., an IAE of 0.104770 and a final-step settling time of 7.59 s. Compared with PID, the IAE is reduced by approximately 74.8% and the final-step settling time by approximately 72.5%.

The robustness study under ±20% variations of the hydropower parameters confirms that the SMC maintains a narrower frequency envelope than PID. Future work should extend the study to nonlinear penstock dynamics, guide-vane rate limits, field-data-based parameter identification and hardware-in-the-loop verification.

REFERENCES

[1]. H. Shayeghi, H. A. Shayanfar, and A. Jalili, "Load frequency control strategies: A state-of-the-art survey for the researcher," Energy Conversion and Management, vol. 50, no. 2, pp. 344-353, 2009. DOI: 10.1016/j.enconman.2008.09.014.

[2]. R. Shankar, S. R. Pradhan, K. Chatterjee, and R. Mandal, "A comprehensive state of the art literature survey on LFC mechanism for power system," Renewable and Sustainable Energy Reviews, vol. 76, pp. 1185-1207, 2017. DOI: 10.1016/j.rser.2017.02.064.

[3]. A. Pappachen and A. P. Peer Fathima, "Critical research areas on load frequency control issues in a deregulated power system: A state-of-the-art-of-review," Renewable and Sustainable Energy Reviews, vol. 72, pp. 163-177, 2017. DOI: 10.1016/j.rser.2016.10.019.

[4]. H. A. Yousef, K. Al-Kharusi, M. H. Albadi, and N. Hosseinzadeh, "Load frequency control of a multi-area power system: An adaptive fuzzy logic approach," IEEE Transactions on Power Systems, vol. 29, no. 4, pp. 1822-1830, 2014. DOI: 10.1109/TPWRS.2013.2297432.

[5]. C. F. Juang and C. F. Lu, "Load-frequency control by hybrid evolutionary fuzzy PI controller," IEE Proceedings - Generation, Transmission and Distribution, vol. 153, no. 2, pp. 196-204, 2006. DOI: 10.1049/ip-gtd:20050176.

[6]. N. Kishor, R. P. Saini, and S. P. Singh, "A review on hydropower plant models and control," Renewable and Sustainable Energy Reviews, vol. 11, no. 5, pp. 776-796, 2007. DOI: 10.1016/j.rser.2005.06.003.

[7]. P. Kundur, Power System Stability and Control. New York, NY, USA: McGraw-Hill, 1994. URL: https://www.accessengineeringlibrary.com/content/book/9780070359581.

[8]. K. Kumar and R. P. Saini, "A review on operation and maintenance of hydropower plants," Sustainable Energy Technologies and Assessments, vol. 49, Article 101704, 2022. DOI: 10.1016/j.seta.2021.101704.

[9]. V. I. Utkin, "Variable structure systems with sliding modes," IEEE Transactions on Automatic Control, vol. 22, no. 2, pp. 212-222, 1977. DOI: 10.1109/TAC.1977.1101446.

[10]. K. D. Young, V. I. Utkin, and U. Ozguner, "A control engineer's guide to sliding mode control," IEEE Transactions on Control Systems Technology, vol. 7, no. 3, pp. 328-342, 1999. DOI: 10.1109/87.761053.

[11]. C. Edwards and S. K. Spurgeon, Sliding Mode Control: Theory and Applications. London, UK: Taylor & Francis, 1998. URL: https://doi.org/10.1201/9781482290801.

[12]. A. Levant, "Sliding order and sliding accuracy in sliding mode control," International Journal of Control, vol. 58, no. 6, pp. 1247-1263, 1993. DOI: 10.1080/00207179308923053.

[13]. Y. Shtessel, C. Edwards, L. Fridman, and A. Levant, Sliding Mode Control and Observation. New York, NY, USA: Birkhauser, 2014. DOI: 10.1007/978-0-8176-4893-0.

[14]. H. K. Khalil, Nonlinear Systems, 3rd ed. Upper Saddle River, NJ, USA: Prentice Hall, 2002. URL: https://www.pearson.com/en-us/subject-catalog/p/nonlinear-systems/P200000003188.

[15]. J. J. E. Slotine and W. Li, Applied Nonlinear Control. Englewood Cliffs, NJ, USA: Prentice Hall, 1991. URL: https://www.worldcat.org/isbn/9780130408907.

[16]. Q. Yang, J. Qian, J. Li, Y. Zou, D. Tian, Y. Zeng, Y. Long, and G. Zhang, "A new integral sliding mode control for hydraulic turbine governing systems based on nonlinear disturbance observer compensation," Sustainability, vol. 15, no. 17, Article 12810, 2023. DOI: 10.3390/su151712810.

[17]. Z. Chen, X. Yuan, Y. Yuan, X. Lei, and B. Zhang, "Parameter estimation of fuzzy sliding mode controller for hydraulic turbine regulating system based on HICA algorithm," Renewable Energy, vol. 133, pp. 551-565, 2019. DOI: 10.1016/j.renene.2018.10.040.

[18]. Z. Chen, X. Yuan, X. Wu, Y. Yuan, and X. Lei, "Global fast terminal sliding mode controller for hydraulic turbine regulating system with actuator dead zone," Journal of the Franklin Institute, vol. 356, no. 15, pp. 8366-8387, 2019. DOI: 10.1016/j.jfranklin.2019.08.006.

[19]. T. Yang, B. Wang, and P. Chen, "Design of a finite-time terminal sliding mode controller for a nonlinear hydro-turbine governing system," Energies, vol. 13, no. 3, Article 634, 2020. DOI: 10.3390/en13030634.

[20]. Y. Tian, B. Wang, P. Chen, and Y. Yang, "Finite-time Takagi-Sugeno fuzzy controller design for hydraulic turbine governing systems with mechanical time delays," Renewable Energy, vol. 173, pp. 614-624, 2021. DOI: 10.1016/j.renene.2021.04.003.

[21]. A. H. Samba, A. Y. Tamtsia, L. N. Nneme, and K. Korassai, "Robust controller for Kaplan hydroturbine governor system based on fast terminal sliding mode control," European Journal of Engineering and Technology Research, vol. 5, no. 8, pp. 922-929, 2020. DOI: 10.24018/ejeng.2020.5.8.2024.

[22]. K. Korassai, A. H. Samba, A. Y. Tamtsia, and L. N. Nneme, "Robust adaptive generalized predictive control with multiple reference model for frequency control in hydroelectric power plants," European Journal of Engineering and Technology Research, vol. 5, no. 8, pp. 930-937, 2020. DOI: 10.24018/ejeng.2020.5.8.2029.

[23]. D. Qian and L. Yu, "Governor design for hydropower plants by intelligent sliding mode variable structure control," Journal of AI and Data Mining, vol. 4, no. 1, pp. 85-92, 2016. DOI: 10.5829/idosi.JAIDM.2016.04.01.10.

[24]. W. Tan, "Unified tuning of PID load frequency controller for power systems via internal model control," IEEE Transactions on Power Systems, vol. 25, no. 1, pp. 341-350, 2010. DOI: 10.1109/TPWRS.2009.2036463.

[25]. S. Debbarma, L. C. Saikia, and N. Sinha, "Automatic generation control using two degree of freedom fractional order PID controller," International Journal of Electrical Power & Energy Systems, vol. 58, pp. 120-129, 2014. DOI: 10.1016/j.ijepes.2014.01.001.

[26]. M. Gheisarnejad and M. H. Khooban, "Design an optimal fuzzy fractional proportional integral derivative controller with derivative filter for load frequency control in power systems," Transactions of the Institute of Measurement and Control, vol. 41, no. 9, pp. 2563-2581, 2019. DOI: 10.1177/0142331218803563.
[27]. V. Veerasamy, N. I. Abdul Wahab, R. Ramachandran, A. Vinayagam, M. L. Othman, H. Hizam, and J. Satheeshkumar, "Automatic load frequency control of a multi-area dynamic interconnected power system using a hybrid PSO-GSA-tuned PID controller," Sustainability, vol. 11, no. 24, Article 6908, 2019. DOI: 10.3390/su11246908.
[28]. M. H. Khooban, T. Niknam, F. Blaabjerg, and T. Dragičević, "A new load frequency control strategy for micro-grids with considering electrical vehicles," Electric Power Systems Research, vol. 143, pp. 585-598, 2017. DOI: 10.1016/j.epsr.2016.10.057.
[29]. M. H. Khooban, T. Dragičević, F. Blaabjerg, and M. Delimar, "Shipboard microgrids: A novel approach to load frequency control," IEEE Transactions on Sustainable Energy, vol. 9, no. 2, pp. 843-852, 2018. DOI: 10.1109/TSTE.2017.2763605.
[30]. S. Saxena and Y. V. Hote, "Load frequency control in power systems via internal model control scheme and model-order reduction," IEEE Transactions on Power Systems, vol. 28, no. 3, pp. 2749-2757, 2013. DOI: 10.1109/TPWRS.2013.2245349.
[31]. J. Machowski, J. W. Bialek, and J. R. Bumby, Power System Dynamics: Stability and Control, 2nd ed. Hoboken, NJ, USA: Wiley, 2008. URL: https://doi.org/10.1002/9781119965056.
[32]. IEEE Power & Energy Society, "IEEE recommended practice for excitation system models for power system stability studies," IEEE Std 421.5-2016, 2016. DOI: 10.1109/IEEESTD.2016.7553421.